

Failure Analysis on Resistive Opens with Scanning SQUID Microscopy

J. Gaudestad, A. Orozco, E.Talanova, L.A. Knauss

Neocera, Inc., 1000 Virginia Manor Road, Beltsville, MD 20705
Tel: 301-210-1010 Fax: 301-210-1042 Email: gaudestad@neocera.com

S. K. Hsiung, K. V. Tan, A. J. Komrowski, D. J. D. Sullivan

LSI Logic Corporation, 3098 West Warren Avenue, Fremont, California 94539
Tel: 408-433-8838 Fax: 408-433-8892 Email: stevehs@lsil.com

Abstract

Scanning Super-conducting Quantum Interference Device (SQUID) Microscopy, also known as SSM, is a current density imaging technique that has been used in failure analysis to localize package- and die-level shorts [1, 2]. New developments have extended this technology to localizing resistive opens, augmenting other non-destructive failure analysis tools like TDR and assisting destructive deprocessing by further pin pointing defect locations. A new method to isolate resistive opens with Scanning SQUID microscopy will be presented in this paper. Also, this paper will illustrate the use of the technique to isolate actual resistive open yield failures in both wire-bond and flip-chip devices.

Introduction

As integrated circuit packages become more complicated, the localization of defects becomes correspondingly more difficult. One particularly difficult class of defects to localize is high resistance defects (HR). These defects include cracked traces, delaminated vias, C4 non-wet defects, Plated Through Hole (PTH) cracks, and any other package or interconnect structure that results in a signal line resistance change that exceeds the specification of the device, but does not result in a complete open. These defects can result in devices that do not run at full speed, are not reliable in the field, or simply do not work at all. The main approach for localizing these defects today is Time Domain Reflectometry (TDR). TDR sends an incident voltage step pulse into the device and monitors the time to receive the reflected waveform. These reflections can correspond to shorts, opens, bends in a wire, normal interfaces between devices, or high resistance defects.

Ultimately anything that produces an electrical impedance change will produce a TDR response. These signals are compared to a known good device and require time consuming layer-by-layer deprocessing and comparison to a standard part. When complete, the best attainable localization of the defect is to within 200 μ m.

A new approach of isolating high resistance defects has been recently developed using current imaging. In recent years, current imaging through magnetic field detection has become a mainstream approach for short localization in the package [1] and is also heavily utilized for die level applications [2]. This core technology has been applied to the localization of high resistance defects. This paper will describe the approach, and give examples of actual resistive open yield failures in both wire-bond and Flip-chip devices at the die-level and interconnect-level respectively.

All studies were conducted on the Magma C20 Scanning SQUID Microscope (SSM) (Figure 1).

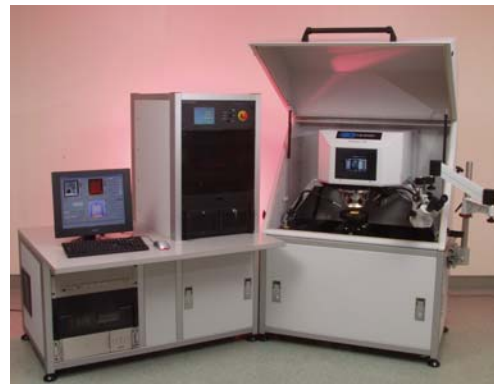


Figure 1 Optical photo of Magma C20 Scanning SQUID Microscope (SSM)

Experimental

The HR defect will force the current in the failing circuit element to follow a slightly different path than in the good part. As we know, a current will create a magnetic field around it. The spatial magnetic field distribution depends on the current distribution itself. Because of the different current distribution in the failing part, there will be a slightly different magnetic field distribution that will be more noticeable in the proximity of the defect. In any case, the differences are expected to be very small. The basic procedure then is to scan the good and failing parts, acquiring the magnetic images of both structures. Because the magnetic differences are very weak in intensity, we cannot see the differences just by looking at the two images; an Image Difference Analysis (IDA) tool has been developed by Neocera to help detect these magnetic anomalies. The shape of the magnetic anomaly depends on both the defect geometry and surrounding circuit elements. Without loss of generality, we can expect to find a “peak” or a “dipole-like” anomaly. For the technique to work, the scan areas to be compared must be the same, requiring precise automated control of set up and data acquisition, provided by the Magma C20 System. Also, differences other than those coming from the defect (for example, misalignments, working distance, manufacturing tolerances, warping, etc.) need to be identified and removed from the resulting image. This is an integral part of the IDA algorithm.

Case Study I: Wire-bond Devices

Background

A wire-bond device with daisy-chain die failed electrical test due to a resistive open. The resistance between the failing daisy-chain pair is as follows (Table 1).

Daisy Chain Pair	Failing Part (Ohms)	Good Part (Ohms)
Pin #96-98	42	3.6

Table 1 Measurement of resistance on the daisy-chain pairs in the failing and good parts

Acoustic Microscope in C-Mode (C-SAM) analysis shows a possible die crack on the die surface (Figure 2).

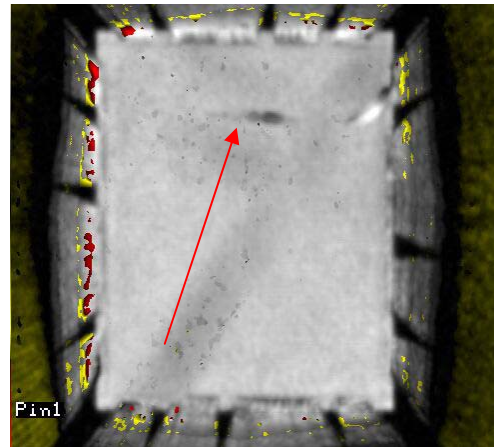


Figure 2 C-SAM image of a possible die crack on the die surface

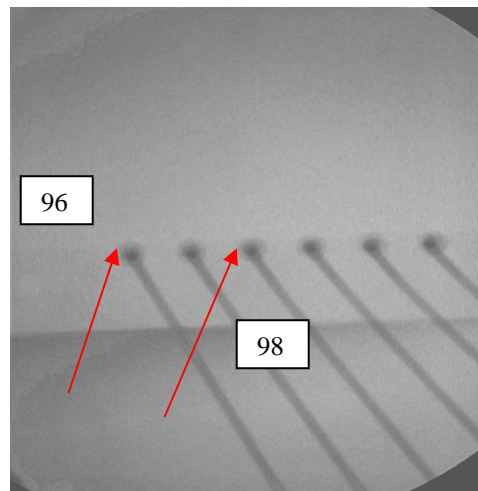


Figure 3 X-ray image of the ball bond of the failing pin# 96 and pin# 98 no anomalies observed.

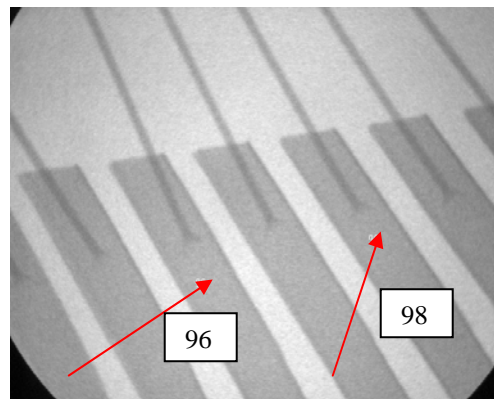


Figure 4 X-ray image of stitch bond of the failing pin#96 and pin#98 no anomalies observed.

Real-time X-ray Inspection observed no anomalies, so an alternative non-destructive approach-using SSM analysis was employed.

Sample Preparation

In order to improve image resolution, some sample preparation is necessary. The mold compound on the wire-bond device was lapped down to the top of the bond wire loop for the failing and good parts. Wires were soldered to the solder balls of the pin #96 and pin #98 in both failing and good parts.

Defect Localization

The failing and good parts were then each sequentially put in the SSM probe station. An AC current of 1.48mA was applied to Pin#96 and Pin#98 in both parts. The distance from the SQUID window to the package surface was 50 μ m. Since the mold compound was partially removed the distance from the SQUID window to the die surface was approximately 430 μ m.

The magnetic-field images picked up by SQUID from the failing and good parts contain only subtle differences (Figure 5 and Figure 6).

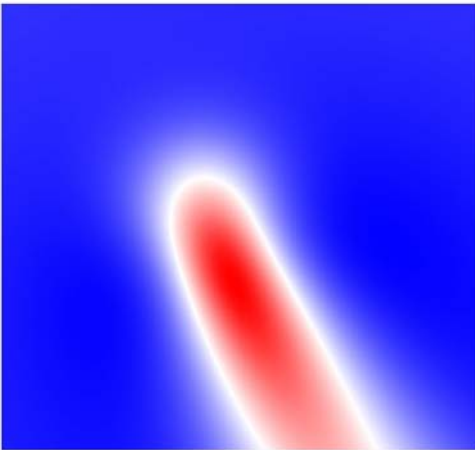


Figure 5 The magnetic-density image of Pin #96 and Pin#98 from the failing part

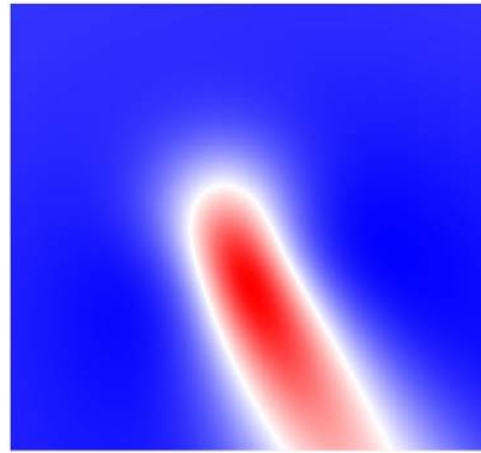


Figure 6 The magnetic-density image of Pin #96 and Pin#98 from the good part.

IDA-Image-processing algorithms are able to optimize the magnetic field comparison of good and failing parts and extract the magnetic anomaly (dipole). The software computes the centroid of the anomaly pointing to the most likely resistive open location (Figure 7 and Figure 8).

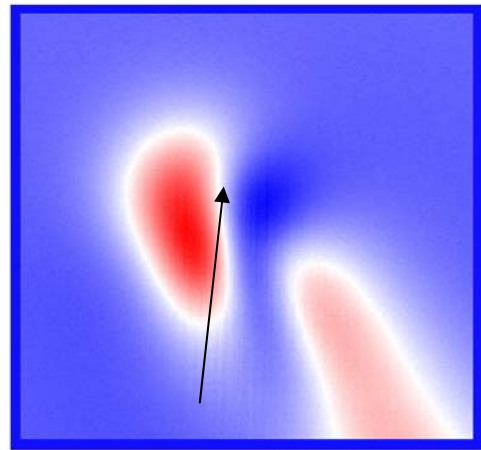


Figure 7 IDA optimized magnetic field comparison showing dipole. The centroid of it is the defect location.

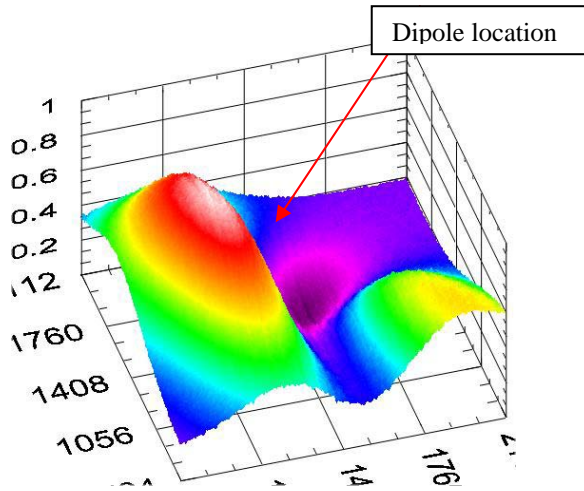


Figure 8 3D of view of IDA residual anomaly

Next a Fast Fourier Transform (FFT) is used to convert the magnetic-field image of Figure 6 into a current-density image [3]. The failing area is easily visualized by overlaying the current density image and the subtracted image dipole center with the X-ray image (Figure 9).

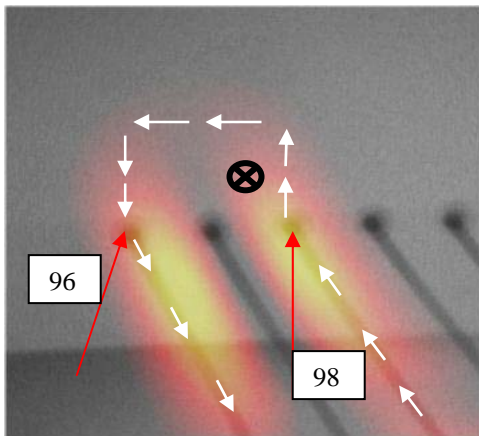


Figure 9 The current-density image overlaid to X-ray image indicates that the resistive open occurred near Pin#98. Also shown is the current path and direction.

Defect Validation

SSM analysis showed that the resistive open occurred within the die metallization, specifically pinpointing the defect to pin #98 prior to any destructive deprocessing.

In order to confirm the SQUID data, the mold compound was further lapped to cut bond wires to isolate the die and the package. Electrical probing confirmed that the resistive open was on the die side of the cut bond wire. On this daisy-chain die,

electrical probing alone was unable to determine the exact location of the failed resistive open.

In order to visually inspect the die surface, the remaining encapsulant was removed with fuming Sulfuric Acid. Optical inspection showed a crack crossing the die surface that broke the top metalization between daisy-chain pair #96-98. The failing area is near Pin#98, confirming what the SSM reported (Figure 10).

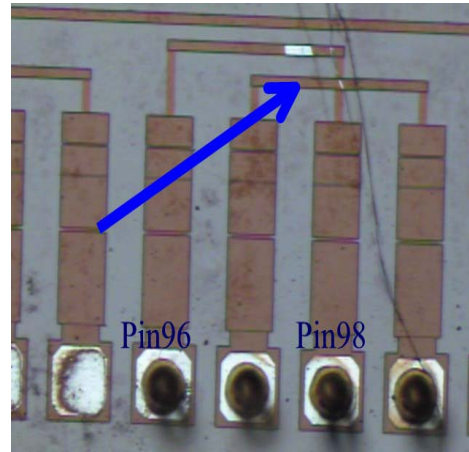


Figure 10 Optical image of die crack that broke the top metalization

Case Study II: Flip-chip Devices

Background

A Flip-chip device with daisy-chain die failed electrical test. The resistance in the failing daisy-chain pair is as follows: (Table 2).

Daisy-chain Pair	Failing Part (Ohms)	Good Part (Ohms)
E4-F4	21	1.93

Table 2 Measurement of resistance on the daisy-chain pairs in the failing and good parts

Acoustic Microscope in C-Mode (C-SAM) analysis showed corner delamination and/or voiding at the die-underfill interface (Figure 11).

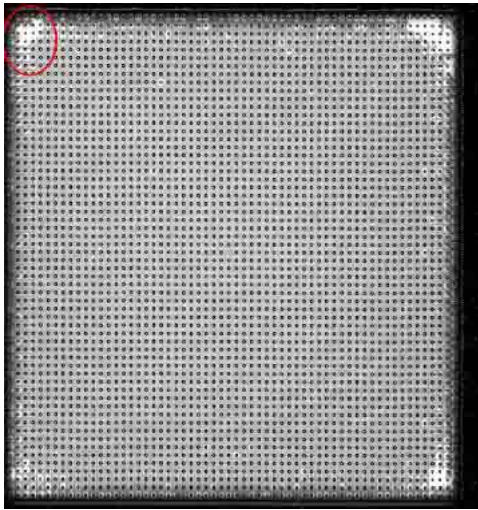


Figure 11 C-SAM image of corner delamination/void at the die-underfill interface. The failing area is indicated with a circle. Corner delamination and/or voiding was seen in all four corners, but the failing pins were confined to only one corner. Time Domain Reflectometry (TDR) analysis was performed to characterize the discontinuity (Figure 12 and Figure 13).

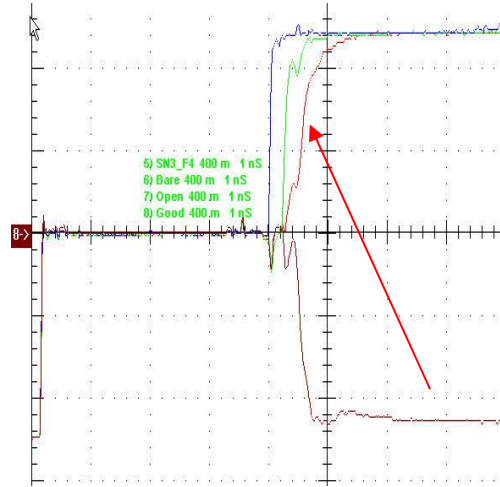


Figure 13 TDR waveforms of pin F4 that indicates it was open in the interconnect solder bump

The TDR waveforms characterized the resistive opens to be in the interconnect solder bumps, but could not specify which solder bumps were failing. Therefore, SSM analysis was used to further localize the defect.

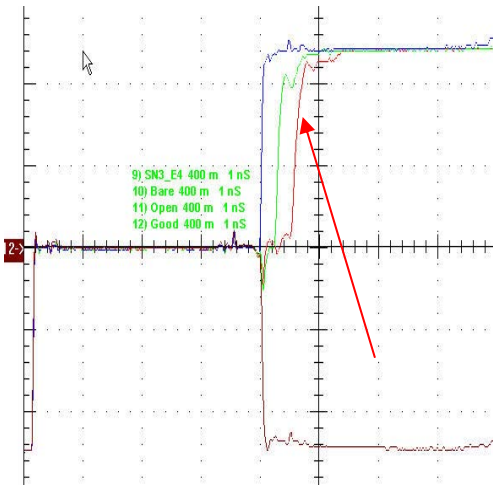


Figure 12 TDR waveforms of pin E4 that indicates it was open in the interconnect solder bump

Sample Preparation

For Flip-chip devices, the die needs to be thinned down to about $100\mu\text{m}$ in order to improve image resolution. Both the failing and good parts were prepared in the same way. The dies were then polished and an anti-reflective coating applied in order to improve the infrared (IR) images. Wires were soldered to the solder balls of pin E4 and F4 on the failing and good parts.

Defect Localization

The failing and good parts were then put in the SSM probe station sequentially. An AC current of 1.48mA was applied to the daisy-chain pair E4-F4.

Similar to the previous described results for Wire-bond devices, the magnetic-density images recorded by SQUID for the failing and good parts appear no different to the unaided human eye (Figure 14 and Figure 15).

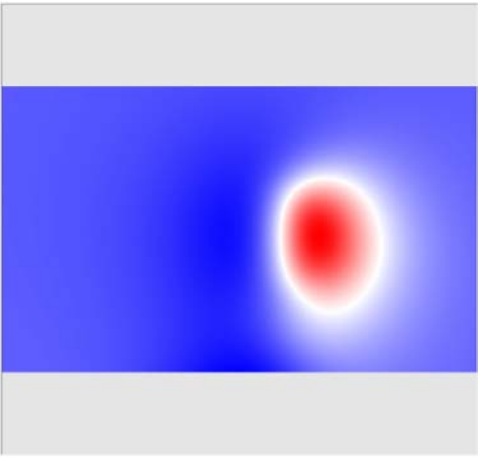


Figure 14 The magnetic images of pinE4 and pinF4 from the failing part

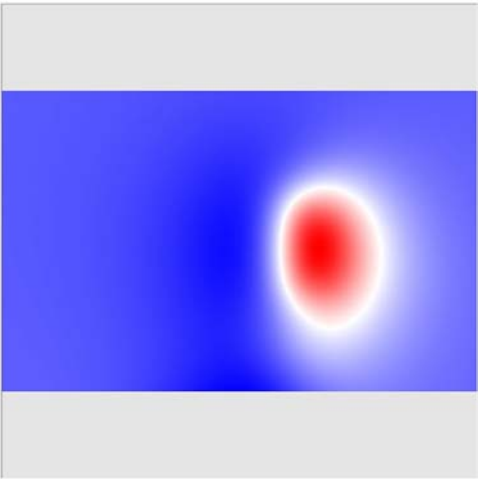


Figure 15 The magnetic images of pin E4 and pin F4 from the good part

Again, IDA image-processing algorithms show a dipole. The center of the dipole is where the resistive open is located (Figure 16 and Figure 17).

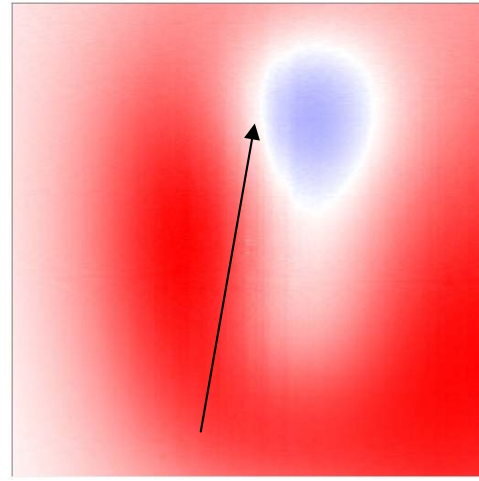


Figure 16 IDA resulting image from the failing and good parts. The centroid of the dipole corresponds to the defect location.

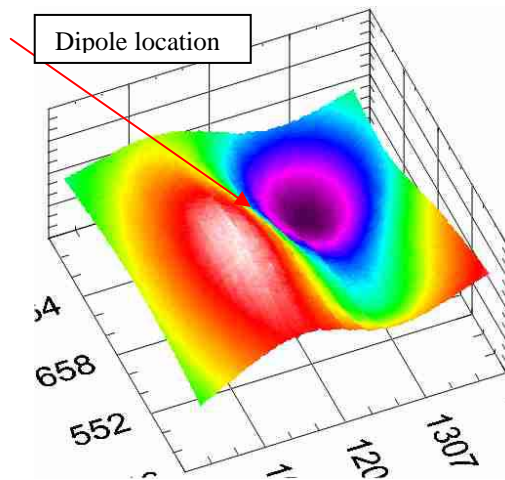


Figure 17 3D of the IDA magnetic field image

The peak image and the magnetic-field IDA image were overlaid with the high resolution IR image. The dipole is very close to the upper solder bump #186 of pin F4. This is the failing location (Figure 18).

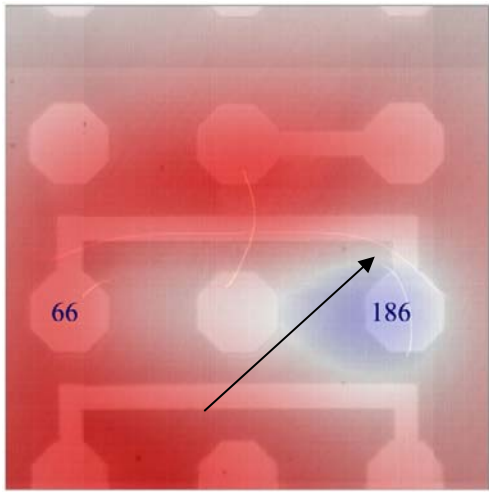


Figure 18 The peak image and the magnetic image were overlaid to the high resolution IR image. The dipole marked with an X is the failing location. (The image has been rotated compared to Figure 16).

Defect Validation

Based on the information from Acoustic Microscope, TDR, and SSM, it is clear that the defect occurred in the solder bump of pin F4.

Mechanical cross-section through the solder bumps of pin E4 and pin F4 revealed a crack in the bump 186 of the pin F4. The crack was caused by solder bump fatigue due to the void at die-underfill interface (Figures 19 to 22). This verifies the SSM defect location.



Figure 19 SEM image of solder bump 186 of pin F4. The crack is indicated by an arrow

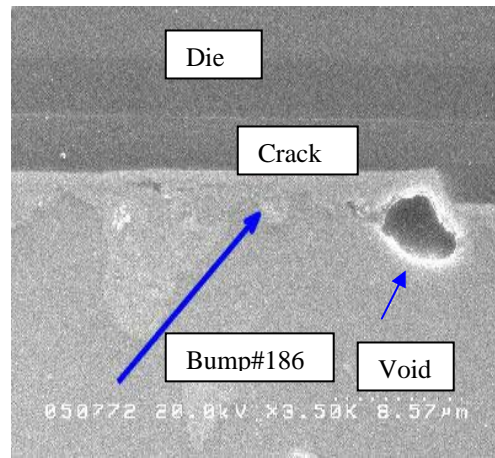


Figure 20 SEM image in high resolution of crack at die-underfill interface in the solder bump #186 of pin F4

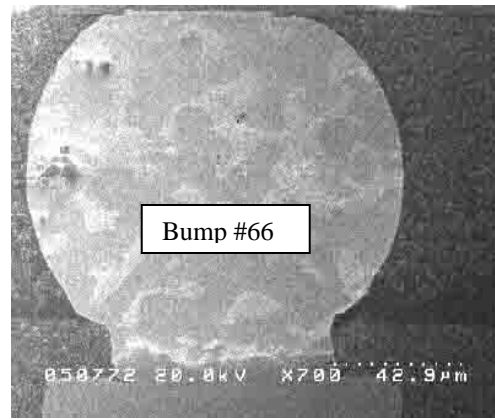


Figure 21 SEM image of good solder bump 66 of Pin E4, which is paired with pin E4

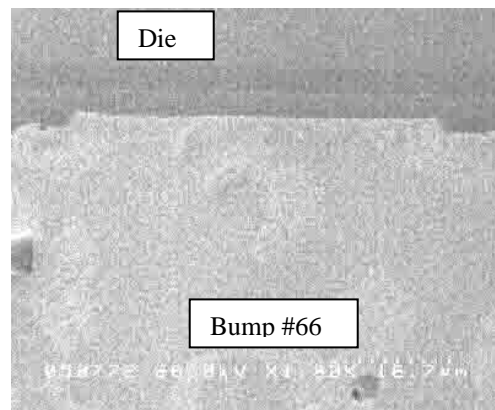


Figure 22 SEM image in high resolution shows good die-underfill interface in the solder bump 66 of pin E4

Summary

Scanning SQUID Microscopy (SSM) has been widely used to locate shorts at the die and package level. Development of new software algorithms allow resistive opens in both Wire-bond and Flip-chip devices to be analyzed. The technique has augmented other non-destructive failure analysis tools and enable more precise localization without destructive deprocessing. Case Studies have proven the technique to successfully locate resistive opens.

Acknowledgements

The authors would like to thank their colleagues at LSI Logic and Neocera for their support in the failure analysis of these parts and the development of this technique.

References

- [1] R. Dias, L Skoglund, Z. Wang, and D. Smith, Integration of SQUID microscopy into FA flow, Proceedings of 27th International Symposium for Testing and Failure Analysis, 77-81 (2001)
- [2] D. Vallett, Scanning SQUID Microscopy for die level fault isolation, Proceedings of 28th International Symposium for Testing and Failure Analysis, 391-396 (2002).
- [3] L.A. Knauss, B.M Frazier, et al., Detecting Power Shorts from the front and backside of IC packages using Scanning SQUID Microscopy, Proceedings of 25th International Symposium for Testing and Failure Analysis, 11-61 (1999)
- [4] A.Orozco, Fault Isolation of High Resistance Defects using Comparative Magnetic Field Imaging, Proceedings of 29th International Symposium for Testing and Failure Analysis, p 9-13 (2003)